Synthesis and Characterization of Dinuclear Metal *σ*-Acetylides and Mononuclear Metal *σ*-Allenylidenes

Michael C. B. Colbert,[†] Jack Lewis,[†] Nicholas J. Long,*[,‡] Paul R. Raithby,[†] Muhammad Younus,[‡] Andrew J. P. White,[‡] David J. Williams,[‡] Nicholas N. Payne,[§] Lesley Yellowlees,[§] David Beljonne,[∥] Nazia Chawdhury,[⊥] and Richard H. Friend[⊥]

Department of Chemistry, University of Cambridge, Lensfield Road, Cambridge CB2 1EW, U.K., Department of Chemistry, Imperial College of Science, Technology and Medicine, South Kensington, London SW7 2AY, U.K., Department of Chemistry, University of Edinburgh, West Mains Road, Edinburgh EH9 3JJ, U.K., Chimie des Materiaux Nouveaux, Université de Mons, Place du Parc, 20, B-7000 Mons, Belgium, and Cavendish Laboratory, University of Cambridge, Madingley Road, Cambridge CB3 0HE, U.K.

Received February 21, 1997

A series of dinuclear metal *σ*-acetylides of the type *trans*-[Cl(P−P)$_2$MC≡CRC≡CM(P−P)$_2$Cl] (M = Fe, Ru, Os; P−P = 1,2-bis(diphenylphosphino)methane (dppm), 1,2-bis(diethylphosphino)ethane (depe), 1,2-bis(dimethylphosphino)ethane (dmpe); R = 1,4-benzenediyl, 1,3-benzenediyl, 2,5-xylenediyl, 2,5-pyridinediyl, 2,5-thiophenediyl) have been formed. Electrochemistry of these complexes shows that there is a metal−metal interaction which is dependent upon the metal and the *π*-conjugated bridging ligand. Coulometry and optical absorbance spectroscopic studies show the presence of mixed-valence oxidized species which possess a delocalized allenylidene structure and can be classified as Robin and Day "class II" mixed-valence species. Theoretical calculations have been carried out to optimize the geometric structure of the bridging acetylide ligand and indicate that the conjugated system undergoes a structural change upon oxidation to give a quinoid-like geometry. Two mononuclear metal−allenylidene complexes, [Cl(dppm)$_2$M=C=C=CHPh][PF$_6$] (**10**, M = Ru; **11**, M = Os), have also been synthesized and an X-ray crystal structure determination on **10** undertaken. This shows a distorted-octahedral coordination about ruthenium and distinct double-bond character extending along the M−C−C−C chain, which is essentially linear. Structural and spectroscopic details on the metal allenylidenes have been compared to those of the mixed-valence oxidized dinuclear metal acetylides and show that the latter exist in a delocalized allenylidene form.

Introduction

The development of synthetic routes toward organometallic metal−acetylide oligomers and polymers has progressed rapidly following the initial reports on group 10 metal−acetylide polymers.[1] Since then, there has been a burgeoning range of ligands and metals incorporated into these ligand systems.[2] The driving force behind these synthetic developments has been the requirement for new products for the materials industry, and these linear, delocalized species are potentially liquid crystalline,[3] conductive (with electron transfer),[4] and third-order nonlinear optical materials.[5] Compounds need to be processible and characterizable, and it is clear that greater variation needs to be introduced

[†] Department of Chemistry, University of Cambridge.
[‡] Department of Chemistry, Imperial College of Science, Technology and Medicine.
[§] Department of Chemistry, University of Edinburgh.
[∥] Chimie des Materiaux Nouveaux, Université de Mons.
[⊥] Cavendish Laboratory, University of Cambridge.

(1) (a) Takahashi, S.; Kariya, M.; Yatuke, K.; Sonogashira, K.; Hagihara, N. *Macromolecules* **1978**, *11*, 1603. (b) Sonogashira, K.; Yatake, T.; Toda, Y.; Takahashi, S.; Hagihara, N. *J. Chem. Soc., Chem. Commun.* **1977**, 291. (c) Sonogashira, K.; Fujikura, Y.; Yatake, T.; Toyoshima, N.; Takahashi, S.; Hagihara, N. *J. Organomet. Chem.* **1978**, *145*, 101. (d) Hagihara, N.; Sonogashira, K.; Takahashi, S. *Adv. Polym. Sci.* **1981**, *41*, 151.

(2) For a recent review on main-group- and transition-metal-based polymers, consult: Manners, I. *Angew. Chem.* **1996**, *108*, 1712; *Angew. Chem., Int. Ed. Engl.* **1996**, *35*, 1602.

(3) (a) Dembek, A. A.; Burch, R. R.; Feiring, A. E. *J. Am. Chem. Soc.* **1993**, *115*, 2087. (b) Altmann, M.; Bunz, U. H. F. *Angew. Chem.* **1995**, *107*, 603; *Angew. Chem., Int. Ed. Engl.* **1995**, *34*, 569. (c) Altmann, M.; Enkelmann, V.; Lieser, G.; Bunz, U. H. F. *Adv. Mater.* **1995**, *7*, 716. (d) Altmann, M.; Bunz, U. H. F. *Macromol. Rapid Commun.* **1994**, *15*, 785. (e) Altmann, M.; Bunz, U. H. F. *Adv. Mater.* **1995**, *7*, 726. (f) Oriol, L.; Serrano, J. L. *Adv. Mater.* **1995**, *7*, 248.

(4) (a) Bunz, U. H. F. *Angew. Chem.* **1994**, *106*, 1127; *Angew. Chem., Int. Ed. Engl.* **1994**, *33*, 1073. (b) Bunz, U. H. F.; Enkelmann, V. *Organometallics* **1994**, *13*, 3823. (c) Bunz, U. H. F.; Wiegelmann-Kreiter, J. E. C. *Chem. Ber.* **1996**, *129*, 785 and references therein. (d) Diederich, F.; Rubin, Y. *Angew. Chem.* **1992**, *104*, 1123; *Angew. Chem., Int. Ed. Engl.* **1992**, *31*, 1101. (e) Diederich, F. In *Modular Chemistry*; NATO ASI Series; Michl, J., Ed.; Kluwer Academic: Dordrecht, The Netherlands, 1996. (f) Diederich, F. In *Modern Acetylene Chemistry*; Stang, P. J., Diederich, F., Eds.; VCH: Weinheim, Germany, 1995; p 443. (g) Diederich, F. *Nature* **1994**, *369*, 149. (h) Benniston, A. C.; Goulle, V.; Harriman, A.; Lehn, J.-M.; Marczinke, B. *J. Phys. Chem.* **1994**, *98*, 7798. (i) Sessler, J. L.; Wang, B.; Harriman, A. *J. Am. Chem. Soc.* **1995**, *117*, 704. (j) Harriman, A.; Odobel, F.; Sauvage, J.-P. *J. Am. Chem. Soc.* **1995**, *117*, 9461. (k) Belser, P.; Dux, R.; Baak, M.; De Cola, L.; Balzani, V. *Angew. Chem.* **1995**, *107*, 634; *Angew. Chem., Int. Ed. Engl.* **1995**, *34*, 595. (l) Grosshenny, V.; Harriman, A.; Ziessel, R. *Angew. Chem.* **1995**, *107*, 1211; *Angew. Chem., Int. Ed. Engl.* **1995**, *34*, 1100. (m) Crossley, M. J.; Burn, P. L.; Langford, S. J.; Prashar, K. *J. Chem. Soc., Chem. Commun.* **1995**, 1921.

S0276-7333(97)00130-1 CCC: $15.00
Publication on Web 06/05/1998

into the π-conjugated bi- or multimetallic systems,[6] *e.g.* incorporation of metals of different oxidation state and variation of phosphines (the bulkier the phosphine, the greater the solubility of the polymer). Our group has recently formed species featuring d^6, d^7, and d^8 metals in order to increase the flexibility of the systems.[7]

Although the bulk physical properties of many organometallic metal−acetylide polymers have been measured, it is instructive to examine the properties of the metals and ligands in the smaller monomeric and oligomeric units[8] and the currently important mixed-valence compounds.[9] This allows greater insight into the synergistic interactions between the metals and ligands in each complex and helps the design of new systems for realistic applications and molecular devices.[10] We can now report the syntheses of dinuclear metal σ-acetylides and mononuclear metal σ-allenylidenes of the iron triad. The bridging acetylide ligands were manipulated so as to vary the interaction between the metal centers, and the mixed-valence dinuclear $M^{II}M^{III}$ complexes were electrosynthesized in order to study their electronic spectra. Treatment of the electrochemical data and the electronic absorption energies by the Hush theory[11] allows the complexes to be classified according to the Robin and Day mixed-valence classification.

Scheme 1. Synthesis of $[Cl(P-P)_2Fe^{II}(C{\equiv}CRC{\equiv}C)Fe^{II}(P-P)_2Cl]$ (3a,c)

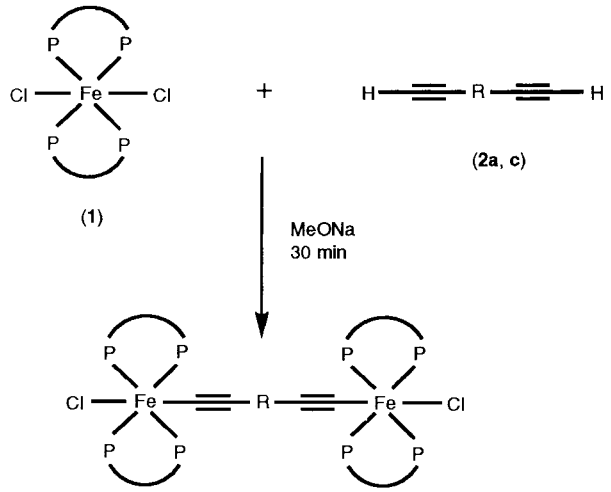

Results and Discussion

Synthesis. The dinuclear complexes synthesized were of the type $[Cl(P-P)_2M^{II}C{\equiv}CRC{\equiv}CM^{II}(P-P)_2Cl]$ (M = Fe, P−P = 1,2-bis(diethylphosphino)ethane (depe), 1,2-bis(dimethylphosphino)ethane (dmpe), R = aromatic spacer group; M = Ru, Os, P−P = 1,2-bis(diphenylphosphino)methane (dppm), R = aromatic spacer group). The iron dinuclear complexes $[Cl(P-P)_2Fe^{II}C{\equiv}CRC{\equiv}CFe^{II}(P-P)_2Cl]$ (**3a**, R = 1,4-substituted benzene, P−P = depe; **3c**, R = 2,5-substituted xylene, P−P = dmpe) were synthesized by modification of a literature procedure[12] (Scheme 1). This synthesis required a very high purity of metal and ligand precursors, as a metal to ligand ratio of 2:1 was essential. The complexes were isolated as

(5) (a) Blau, W. J.; Byrne, H. J.; Cardin, D. J.; Davey, A. P. *J. Mater. Chem.* **1991**, *1*, 245. (b) Blau, W. J.; Byrne, H. J.; Cardin, D. J.; Davey, A. P. In *Organic Molecules for Nonlinear Optics and Photonics*; Messier, J., Kajar, F., Prasad, P., Ulrich, D., Eds.; Kluwer Academic: Dordrecht, The Netherlands, 1991; p 391. (c) Long, N. J. *Angew. Chem.* **1995**, *107*, 37; *Angew. Chem., Int. Ed. Engl.* **1995**, *34*, 21. (d) Marder, S. R. In *Inorganic Materials*; Bruce, D. W., O'Hare, D., Eds.; Wiley: New York, 1992; pp 115−164. (e) Frazier, C. C.; Guha, S.; Chen, W. P.; Cockerham, M. P.; Porter, P. L.; Chauchard, E. A.; Lee, C. H. *Polymer* **1987**, *28*, 553. (f) Fyfe, H. B.; Mlekuz, M.; Stringer, G.; Taylor, N. J.; Marder, T. B. In *Inorganic and Organometallic Polymers With Special Properties*; NATO ASI Series E; Laine, R. M., Ed.; Kluwer Academic: Dordrecht, The Netherlands, 1992; Vol. 206, pp 331−344.

(6) (a) Le Narvor, N.; Toupet, L.; Lapinte, C. *J. Am. Chem. Soc.* **1995**, *117*, 7129. (b) Le Narvor, N.; Lapinte, C. *Organometallics* **1995**, *14*, 634. (c) Stang, P. J.; Tykwinski, R. *J. Am. Chem. Soc.* **1992**, *114*, 4411. (d) Weng, W.; Bartik, T.; Gladysz, J. A. *Angew. Chem.* **1994**, *106*, 2272; *Angew. Chem., Int. Ed. Engl.* **1994**, *33*, 2199. (e) Brady, M.; Weng, W.; Gladysz, J. A. *J. Chem. Soc., Chem. Commun.* **1994**, 2655. (f) Fyfe, H. B.; Mlekuz, M.; Zargarian, D.; Taylor, N. J.; Marder, T. B. *J. Chem. Soc., Chem. Commun.* **1991**, 188. (g) Davies, S. J.; Johnson, B. F. G.; Khan, M. S.; Lewis, J. *J. Chem. Soc., Chem. Commun.* **1991**, 187. (h) Khan, M. S.; Schwartz, D. J.; Pasha, N. A.; Kakkar, A. K.; Lin, B.; Raithby, P. R.; Lewis, J. *Z. Anorg. Allg. Chem.* **1992**, *616*, 121. (i) Ingham, S. L.; Khan, M. S.; Lewis, J.; Long, N. J.; Raithby, P. R. *J. Organomet. Chem.* **1994**, *470*, 153. (j) Faulkner, C. W.; Ingham, S. L.; Khan, M. S.; Lewis, J.; Long, N. J.; Raithby, P. R. *J. Organomet. Chem.* **1994**, *487*, 139. (k) Lavastre, O.; Even, M.; Dixneuf, P. H.; Pacreau, A.; Vairon, J.-P. *Organometallics* **1996**, *15*, 1530. (l) Whittal, I. R.; Humphrey, M. G.; Hockless, D. C. R.; Skelton, B. W.; White, A. H. *Organometallics* **1995**, *14*, 3970. (m) Pollagi, T. P.; Stoner, T. C.; Dallinger, R. F.; Gilbert, T. M.; Hopkins, M. D. *J. Am. Chem. Soc.* **1991**, *113*, 703. (n) Myers, L. K.; Langhoff, C.; Thompson, M. E. *J. Am. Chem. Soc.* **1992**, *114*, 7560. (o) Sun, Y.; Taylor, N. J.; Carty, A. J. *J. Organomet. Chem.* **1992**, *423*, C23. (p) Field, L. D.; George, A. V.; Hockless, D. C. R.; Purches, G. R.; White, A. H. *J. Chem. Soc., Dalton Trans.* **1996**, 2011. (q) Chawdhury, N.; Kohler, A.; Friend, R. H.; Younus, M.; Long, N. J.; Raithby, P. R.; Lewis, J. *Macromolecules* **1998**, *31*, 722.

(7) For example: (a) Davies, S. J.; Johnson, B. F. G.; Khan, M. S.; Lewis, J. *J. Chem. Soc., Chem. Commun.* **1991**, 187. (b) Khan, M. S.; Davies, S. J.; Kakkar, A. K.; Schwartz, D. J.; Lin, B.; Johnson, B. F. G.; Lewis, J. *J. Organomet. Chem.* **1992**, *424*, 87. (c) Lewis, J.; Khan, M. S.; Kakkar, A. K.; Raithby, P. R.; Fuhrmann, K.; Friend, R. H. *J. Organomet. Chem.* **1992**, *443*, 135. (d) Khan, M. S.; Pasha, N. A.; Kakkar, A. K.; Raithby, P. R.; Lewis, J.; Fuhrmann, K.; Friend, R. H. *J. Mater. Chem.* **1992**, *2*, 759. (e) Atherton, Z.; Faulkner, C. W.; Ingham, S. L.; Kakkar, A. K.; Khan, M. S.; Lewis, J.; Long, N. J.; Raithby, P. R. *J. Organomet. Chem.* **1993**, *462*, 265. (f) Faulkner, C. W.; Ingham, S. I.; Khan, M. S.; Lewis, J.; Long, N. J.; Raithby, P. R. *J. Organomet. Chem.* **1994**, *482*, 139. (g) Lewis, J.; Long, N. J.; Raithby, P. R.; Shields, G. P.; Wong, W.-Y.; Younus, M. *J. Chem. Soc., Dalton Trans.* **1997**, 4283.

(8) (a) Lavastre, O.; Even, M.; Dixneuf, P. H.; Pacreau, A.; Vairon, J.-P. *Organometallics* **1996**, *15*, 1530. (b) Touchard, D.; Pirio, N.; Toupet, L.; Fettouhi, M.; Ouahab, L.; Dixneuf, P. H. *Organometallics* **1995**, *14*, 5263. (c) Touchard, D.; Pirio, N.; Dixneuf, P. H. *Organometallics* **1995**, *14*, 4920.

(9) For a monograph and comprehensive recent reviews, see: (a) Brown, D. B., Ed. *Mixed-Valence Compounds*; Reidel: Dordrecht, The Netherlands, 1980. (b) Ward, M. D. *Chem. Soc. Rev.* **1995**, 121. (c) Ward, M. D. *Chem. Ind.* **1996**, *Aug*, 568. For examples: (d) Cowan, D. O.; LeVanda, C. *J. Am. Chem. Soc.* **1972**, *94*, 9271. (e) Mueller-Westerhoff, U. T.; Eilbracht, P. *J. Am. Chem. Soc.* **1972**, *94*, 9272. (f) LeVanda, C.; Bechgaard, K.; Cowan, D. O.; Mueller-Westerhoff, U. T.; Eilbracht, P.; Candela, G. A.; Collinns, R. L. *J. Am. Chem. Soc.* **1976**, *98*, 3181. (g) Morrison, W., Jr.; Krogsrud, S.; Hendrickson, D. N. *Inorg. Chem.* **1973**, *12*, 1998. (h) Lee, M.-T.; Foxman, B. M.; Rosenblum, M. *Organometallics* **1985**, *4*, 539. (i) Pittmann, C. U., Jr.; Surynarayanan, B. *J. Am. Chem. Soc.* **1974**, *96*, 7916. (j) Sato, M.; Shintate, H.; Kawata, Y.; Sekino, M.; Katada, M.; Kawata, S. *Organometallics* **1994**, *13*, 1956. (k) Sato, M.; Hayashi, Y.; Shintate, H.; Katada, M.; Kawata, S. *J. Organomet. Chem.* **1994**, *471*, 179. (l) Sato, M.; Mogi, E.; Kamakura, S. *Organometallics* **1995**, *14*, 3157. (m) Colbert, M. C. B.; Ingham, S. L.; Lewis, J.; Long, N. J.; Raithby, P. R. *J. Chem. Soc., Dalton Trans.* **1994**, 2215. (n) Colbert, M. C. B.; Edwards, A. J.; Lewis, J.; Long, N. J.; Page, N. A.; Parker, D. G.; Raithby, P. R. *J. Chem. Soc., Dalton Trans.* **1994**, 2589.

(10) (a) Lehn, J.-M. In *Supramolecular Chemistry: Concepts and Perspectives*; VCH: Weinheim, Germany, 1995. (b) Campagna, S.; Denti, G.; Serroni, S.; Juris, A.; Venturi, M.; Riceunto, V.; Balzani, V. *Chem. Eur. J.* **1995**, *1*, 211.

(11) Hush, N. S. *Prog. Inorg. Chem.* **1967**, *8*, 391.

(12) Field, L. D.; George, A. V.; Laschi, F.; Malouf, E. Y.; Zanello, P. *J. Organomet. Chem.* **1992**, *435*, 347.

Scheme 2. Synthesis of $[Cl(dppm)_2M^{II}(C{\equiv}CRC{\equiv}C)M^{II}(dppm)_2Cl]$ (8a−e, M = Ru; 9a−e, M = Os)

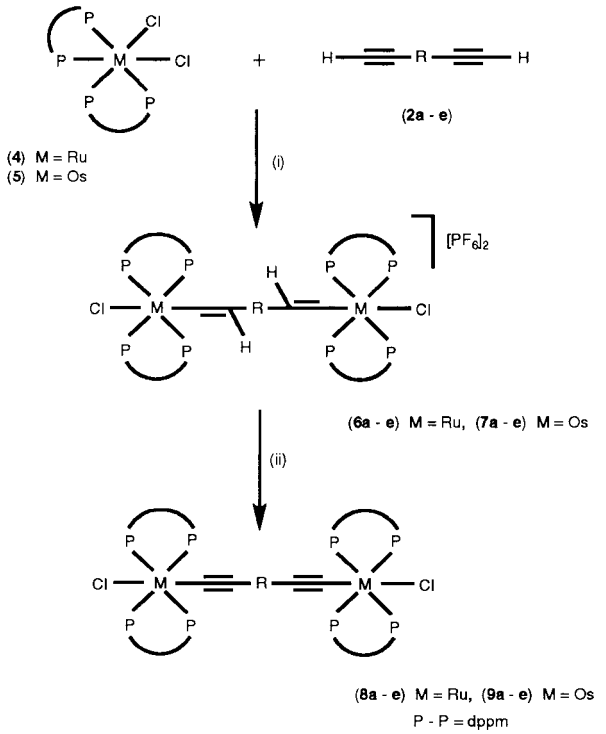

(i) (**4**) or (**5**) 2 equiv., (**2**) 1 equiv., $NaPF_6$ 2 equiv., CH_2Cl_2, r. t., N_2, 8h
(ii) DBU 2 equiv., CH_2Cl_2, r. t., N_2, 8h

brown solids in reasonable yields. Attempts to synthesize other dinuclear iron complexes using different bridging ligands were unsuccessful, as mixtures of products (mono- and dimetal acetylides and mixed-valence species $Fe^{II}-Fe^{III}$) were obtained and could not be separated. Efforts to synthesize the ruthenium and osmium analogues resulted in decomposition of the *trans* metal acetylides, despite using different bidentate phosphine ligands: *e.g.* depe, dmpe, dppm, and dppe (1,2-bis(diphenylphosphino)ethane).

A different synthetic method (illustrated in Scheme 2) afforded the synthesis of ruthenium and osmium dinuclear species featuring various bridging acetylene ligands (**2a**−**e**; Figure 1). However, via this route, the metallic precursor is restricted to being *cis*-$[M(dppm)_2Cl_2]$ (**4**, M = Ru; **5**, M = Os), so that direct comparison with the iron analogues **3a** and **3c** was not possible.

The intermediate vinylidenes **6a**−**e** and **7a**−**e** were not characterized but were purified by filtration before step ii. Complexes **8a**−**d** and **9a**−**d** were isolated as yellow powders in approximately 50% yields, while complexes **8e** and **9e** were also yellow solids, produced in 25% yield.

The mononuclear metal allenylidene complexes **10** and **11** were synthesized from the respective *cis* metal dihalide (**4** or **5**), [(Ph)(OH)HCC≡CH], and $NaPF_6$ and isolated as stable, red solids in excellent yields (Scheme 3). The formation of **10** has been communicated previously,[13] but without any synthetic or structural details. These secondary metal allenylidene species are synthesized via the dehydration of the propargylic alcohol and owe their stability to the delocalization over the terminal phenyl group of the electron density surrounding the multiply bonded carbon chain. Our motivation for the formation of these allenylidenes was to confirm the conjugated nature of the M=C and C=C=C linkages and to relate the structures and spectroscopic details of the novel mixed-valence oxidized dinuclear metal acetylides with those of the allenylidenes.

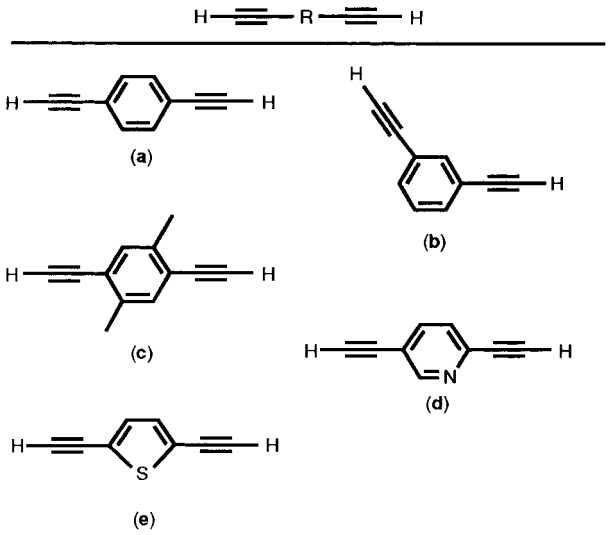

R = (**a**) 1, 4 - benzene, (**b**) 1, 3 - benzene, (**c**) 2, 5 - xylene, (**d**) 2, 5 - pyridine, (**e**) 2, 5 - thiophene

Figure 1. Bridging acetylene ligands used in the dinuclear complexes.

Scheme 3. Synthesis of $[Cl(dppm)_2M{=}C{=}C{=}CHPh][PF_6]$ (10, M = Ru; 11, M = Os)

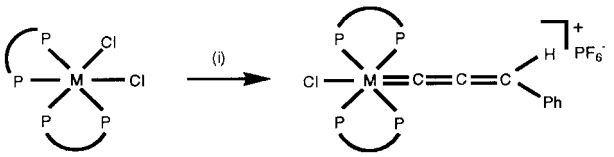

(i) = HC≡CCH(OH)Ph, $NaPF_6$, CH_2Cl_2

By forming a range of dinuclear metal acetylide systems and varying the metal and ligand moieties, it was possible to gain information and insight into the metal−metal interaction. The degree of this interaction through the conjugated bridging ligands was measured by two methods: (i) electrochemical, resulting in the relative comproportionation constant (K_{com}) values of the complexes, and (ii) spectroelectrochemical, yielding the α^2 (H_{AB}^2) delocalization parameter via the Hush theoretical treatment.

X-ray Structure Determination of 10. The structure of **10** was determined by X-ray diffraction techniques. A view of the structure is shown in Figure 2, while selected bond parameters are listed in Table 1. The determination showed **10** to crystallize with two crystallographically independent molecules with overall C_s symmetry in the asymmetric unit, the mirror plane passing through the phosphorus atom and bisecting

(13) Pirio, N.; Touchard, D.; Dixneuf, P. H. *J. Organomet. Chem.* **1993**, *462*, C18.

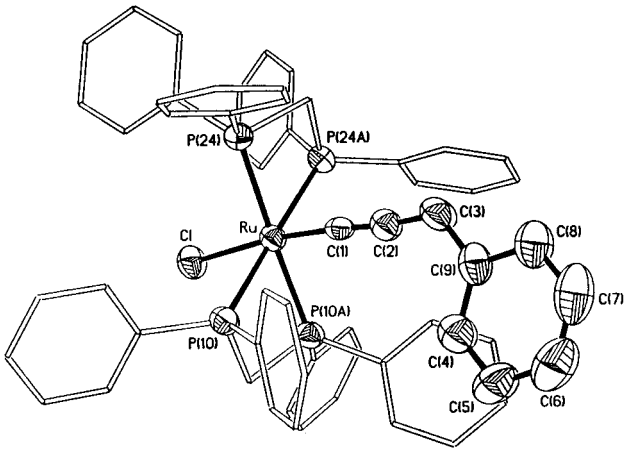

Figure 2. One of the two crystallographically independent C_s-symmetric molecules of $[Cl(dppm)_2Ru(=C=C=CHPh)]^+[PF_6]^-$ present in the structure of **10** (50% probability ellipsoids).

Table 1. Selected Bond Lengths (Å) and Angles (deg) for 10

Ru−C(1)	1.886(10)	Ru−P(10)	2.381(2)
Ru−P(24)	2.383(2)	Ru−Cl	2.460(3)
C(1)−C(2)	1.254(14)	C(2)−C(3)	1.34(2)
C(3)−C(9)	1.42(2)	Ru′−C(1′)	1.874(11)
Ru′−P(10′)	2.371(2)	Ru′−P(24′)	2.395(2)
Ru′−Cl′	2.475(3)	C(1′)−C(2′)	1.239(14)
C(2′)−C(3′)	1.36(2)	C(3′)−C(9′)	1.46(2)
C(1)−Ru−P(10)	91.4(2)	P(10)#1−Ru−P(10)	69.93(9)
P(10)−Ru−P(24)#1	177.36(7)	C(1)−Ru−P(24)	86.0(2)
P(10)−Ru−P(24)	110.39(6)	P(24)#1−Ru−P(24)	69.16(9)
C(1)−Ru−Cl	173.4(3)	P(10)−Ru−Cl	83.17(7)
P(24)−Ru−Cl	99.47(7)	C(2)−C(1)−Ru	177.0(8)
C(1)−C(2)−C(3)	174.1(11)	C(2)−C(3)−C(9)	127.0(10)
C(8)−C(9)−C(3)	119.8(12)	C(4)−C(9)−C(3)	122.9(10)
C(1′)−Ru′−P(10′)	96.5(3)	P(10′)−Ru′−P(10′)#1	69.21(10)
P(10)−Ru′−P(24′)#1	172.29(8)	C(1′)−Ru′−P(24′)	91.2(3)
P(10′)−Ru′−P(24′)	109.73(7)	P(24)#1−Ru′−P(24′)	70.23(11)
C(1′)−Ru′−Cl′	178.3(3)	P(10′)−Ru′−Cl′	84.88(8)
P(24′)−Ru′−Cl′	87.42(8)	C(2′)−C(1′)−Ru′	176.1(10)
C(1′)−C(2′)−C(3′)	175.8(13)	C(2′)−C(3′)−C(9′)	126.1(13)
C(8′)−C(9′)−C(3′)	118.2(14)	C(4′)−C(9′)−C(3′)	122.0(11)

each dppm ligand. Both the chlorine atom and the allenylidene ligand lie within the mirror plane.

The gross conformations of the central coordination sphere and the allenylidene ligand in the two independent molecules are very similar, with the maximum deviation from the best fit being 0.38 Å for the chlorine atom. The coordination at ruthenium is distorted octahedral, with angles at Ru in the range 69.2−110.4 and 173.4−177.4° in molecule 1, and 69.2−109.7 and 172.3−178.3° in molecule 2. The principal contractions from 90° are due to the "bite" of the chelating dppm ligands. The Ru−P bonds are typical at 2.371(2)−2.395(2) Å, while the Ru−Cl distances at 2.460(3) and 2.475(3) Å are slightly lengthened from the expected range for terminal chlorine atoms on octahedral ruthenium. There is a distinct pattern of double-bond character that extends from Ru to C(2), with Ru=C distances of 1.886(10) and 1.874(11) Å and C(1)=C(2) lengths of 1.254(14) and 1.239(14) Å, respectively, for molecules 1 and 2. C(2)=C(3) is notably longer at 1.34(2) and 1.36(2) Å, respectively, and the pattern of delocalization does not extend significantly into the C−aryl bond (1.42(2) and 1.46(2) Å in molecules 1 and 2, respectively, C(3)−C(9)). The Ru−C(1)−C(2)−C(3) chain is very nearly linear with angles at C(1) of 177.0(8) and 176.1(10)° and at C(2) of 174.1(11) and 175.8(13)°, as is also observed in an analogous ruthenium diphenylallenylidene complex.[14] The angles at C(3) are noticeably enlarged from trigonal at 127.0(10) and 126.1(13)°, respectively.

The region surrounding the C(1)−C(2) double bond is fairly unhindered, with the closest approaches being from phosphine *ortho* C−H hydrogen atoms at *ca.* 2.9 Å. There is a similar absence of any approaches in the other independent molecule, though a pair of phosphine *ortho* C−H hydrogen atoms do lie at *ca.* 2.6 Å to the center of the C(1)=C(2) bond. However, approach to the ruthenium allenylidene linkage is effectively blocked by the bulky phosphine rings. This steric protection of the allenylidene linkage by the phenyl groups has also been observed in an analogous ruthenium−allenylidene complex.[15] However, the bond parameters in this latter complex do not warrant close comparison, since the compound crystallizes with two disterically differing conformers of the ruthenium−allenylidene cation.

It is interesting to note that the linear geometry of the acetylenic linkage of the propargylic alcohol is retained upon dehydration and coordination to the ruthenium center, though clearly there are gross changes in the bond order throughout the Ru−C−C−C linkage, thus leading to the allenylidene−metal complex.

Table 2. Electrode Potentials and Comproportionation Constants of Dinuclear Complexes[a]

complex	ΔE_p^I (V)	$E_{1/2}^I$ (V)	ΔE_p^{II} (V)	$E_{1/2}^{II}$ (V)	$\Delta E_{1/2}$ (V)	K_{com}
1 (P−P = depe)	0.06	−0.53				
1 (P−P = dmpe)	0.10	−0.48				
4	0.09	0.09				
5	0.10	−0.22				
8a	0.07	−0.30	0.10	0.00	0.30	1.2×10^5
8b	0.09	−1.20	0.09	0.07	0.19	1.6×10^3
8c	0.08	−0.35	0.09	−0.02	0.33	3.8×10^5
8d	0.08	−0.22	0.10	0.10	0.32	2.5×10^5
8e	0.09	−0.47	0.08	−0.11	0.36	1.2×10^6
9a	0.08	−0.51	0.10	−0.21	0.30	1.2×10^5
9b	0.07	−0.34	0.10	−0.17	0.17	7.5×10^2
9c	0.08	−0.56	0.09	−0.26	0.30	1.2×10^5
9d	0.08	−0.44	0.10	−0.15	0.29	8.0×10^4
9e	0.09	−0.71	0.09	−0.19	0.32	2.6×10^5
3a	0.06	−0.63	0.06	−0.47	0.16	5.1×10^2
3c	0.07	−0.56	0.07	−0.32	0.24	1.3×10^4

[a] All $E_{1/2}$ values are referenced to $FeCp_2$ in the same system; scan rate 100 mV s^{-1}. $E_{1/2}^I$ and $E_{1/2}^{II}$ are the first and second electrode potentials of the dinuclear species. $\Delta E_{1/2} = E_{1/2}^{II} - E_{1/2}^I$.

Electrochemical Properties of Dinuclear Metal Acetylides. Electrochemical measurements were recorded at 298 K in a standard three-electrode cell (platinum working and auxiliary electrodes and an Ag/AgCl reference electrode) using a 0.1 M $[NBu_4][BF_4]/CH_2Cl_2$ solution as electrolyte. The results of the electrochemical experiments are presented in Table 2.

The redox properties of some dinuclear metal acetylides have been reported previously, and there are indications that metal−metal interactions can occur in these dinuclear systems. This interaction can be measured using cyclic voltammetry.[16−18] The system most

(14) Selegue, J. P. *Organometallics* **1982**, *1*, 217.
(15) Pirio, N.; Touchard, D.; Toupet, L.; Dixneuf, P. H. *J. Chem. Soc., Chem. Commun.* **1991**, 980.
(16) Brady, M.; Weng, W.; Gladysz, J. A. *J. Chem. Soc., Chem. Commun.* **1994**, 2655.

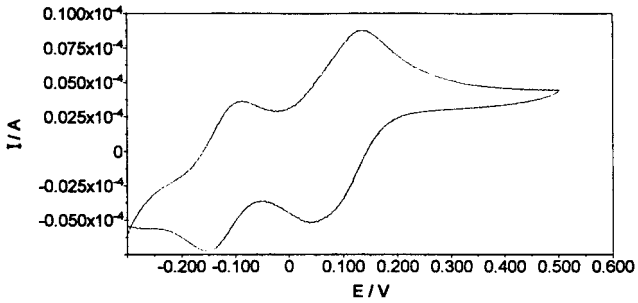

Figure 3. Cyclic voltammogram of $[Cl(dmpe)_2Fe^{II}(C{\equiv}CRC{\equiv}C)Fe^{II}(dmpe)_2Cl]$ (R = 2,5-xylenediyl; **3c**.

Scheme 4. Mechanism for the Two One-Electron Oxidations of a $M^{II}M^{II}$ Complex

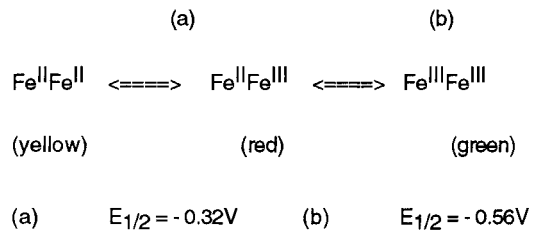

relevant to the dinuclear complexes in this work is $[ClFe^{II}(dmpe)_2(C{\equiv}CRC{\equiv}C)Fe^{II}(dmpe)_2Cl]$ (R = 1,4-benzenediyl) investigated by Field *et al.*[12]

The cyclic voltammogram of our analogous compound **3c** displays two closely spaced, chemically reversible oxidation processes (**I** ($E_{1/2}$ = −0.32 V) and **II** ($E_{1/2}$ = −0.56 V)) separated by 0.24 V (Figure 3). Step-by-step controlled-potential coulometry (E_w = −0.50 and −0.66 V) reveals that each step involves transfer of 1 mol of electrons. During the bulk electrolysis, the color changes from yellow-brown to red and then to green; these colors are associated with the neutral, monocationic, and dicationic species, respectively. This electrochemical behavior is attributed to a metal−metal interaction through the conjugated ligand and can be represented by Scheme 4.

The coupled oxidation waves were found to be on either side of the redox potential for the *trans*-$[Fe(depe)_2Cl_2]$ complex ($E_{1/2}$ = −0.53 V). Substitution of one chloride ligand in this mononuclear precursor by the $C{\equiv}CRC{\equiv}CFe(depe)_2Cl$ unit should result in a positive shift of the $Fe^{II/III}$ redox couple. Subsequently, in **3a**, the observed shift of 0.16 V suggests a small but significant interaction between the two metal centers. The K_{com} value for this complex is derived from $\Delta E_{1/2}$ by eq 1. Its value of 5.1×10^2 suggests that **3a** belongs

$$\log K_{com} = 16.9(\Delta E_{1/2}) \qquad (1)$$

to the Robin−Day "class II" weakly coupled mixed-valence species. These findings are supported by the investigations on the analogous diiron(II) complex.[12] The Robin and Day classification[19] of mixed-valence systems based on the extent of intramolecular interaction features *three* types of species. In compounds of *class I*, no interaction between the two metals exists, and these compounds exhibit properties typical of the independent molecules. Compounds of *class II* feature a moderate degree of interaction so that these compounds possess new properties in addition to those of their components. *Class III* refers to those compounds in which strong interactions between the two metals exist, so that none of the properties of the components remain and a new delocalized species exists.

The redox chemistry of complexes **8a**−**e** and **9a**−**e** is similar to that described above for $[Cl(P{-}P)_2Fe^{II}(C{\equiv}CRC{\equiv}C)Fe^{II}(P{-}P)_2Cl$ (**3a**,**c**); however, the introduction of different metals and ligands into the system significantly changes the degree of metal−metal ($\Delta E_{1/2}$ values) interaction through the π-conjugated bridging ligand.

The cited redox processes are essentially reversible from an electrochemical viewpoint, as confirmed by standard diagnostic tests; for example, (i) ΔE_p = 0.06−0.10 V and (ii) $i_{p,c}/i_{p,a} = 1$ with scan rates varying from 0.05 to 0.5 V s^{-1} (under the same conditions, the one-electron oxidation of ferrocene occurs at +0.50 V, displaying a peak-to-peak separation of 80 mV at 0.1 V s^{-1}). The data in Table 2 show that the $\Delta E_{1/2}$ values vary depending on the metal and bridging ligand in the systems. The consequent variation in K_{com} values suggests that the corresponding mixed-valence species $M^{II}M^{III}$ have different degrees of delocalization between the metal centers. This delocalization can be examined more closely through the optical absorbance spectroscopic studies of the complexes (see later).

Examination of the K_{com} values in Table 2 highlights certain trends. For example, all the ruthenium and osmium binuclear complexes have similar metal−metal interactions apart from those bridged by the 1,3-diethynylbenzene ligand, due to an unfavorable metal−ligand orbital interaction in this species. This agrees with the recent observation that, in analogous systems, the communication between metal centers through a bridging unit is affected by the nature of either the bridge or the terminal metal fragments.[20]

Coulometry of Dinuclear Metal Acetylides. Step-by-step controlled-potential coulometry was used to measure the number of electrons involved in the multiwave redox processes. In each case, two one-electron-transfer steps were observed. Distinct changes in the $\nu(C{\equiv}C)$ stretching frequencies and ultraviolet absorbances of the monocationic ($M^{II}M^{III}$) complexes suggested that metal−bridging ligand interactions were significantly different in the mixed-valence species compared to those in the neutral ($M^{II}M^{II}$) system. The infrared and ultraviolet/visible measurements for the neutral and charged species are presented in Table 3. In the monocationic species, there are two new peaks in the visible region between *ca.* 450 and 600 nm, probably due to ligand-to-metal charge-transfer transitions.[21] The observation of an absorption at the limit between the visible range and near-infrared range for $[\mathbf{3a}]^+$ (Figure 4) and $[\mathbf{3c}]^+$ has also been observed for analogous $Fe^{II}Fe^{III}$ complexes.[21]

(17) Sato, M.; Hayashi, Y.; Shintate, H. *J. Organomet. Chem.* **1994**, *471*, 179.
(18) Etzenhauser, B. A.; DiBiase Cavanagh, M.; Spurgeon, H. N.; Sponsler, M. B. *J. Am. Chem. Soc.* **1994**, *116*, 2221.
(19) Robin, M. B.; Day, P. *Adv. Inorg. Chem. Radiochem.* **1967**, *10*, 247.
(20) Lavastre, O.; Plass, J.; Bachmann, P.; Guesmi, S.; Moinet, C.; Dixneuf, P. H. *Organometallics* **1997**, *16*, 184.
(21) Coat, F.; Guillevic, M.-A.; Toupet, L.; Paul, F.; Lapinte, C. *Organometallics* **1997**, *16*, 5988.

Table 3. Infrared and Ultraviolet Data for the Neutral ($M^{II}M^{II}$) and Mixed-Valence Species ($M^{II}M^{III}$)

	$M^{II}M^{II}$ system			$M^{II}M^{III}$ system		
complex	IR ν(C≡C) (cm^{-1})	UV/vis (nm)	color	IR ν(C=C) (cm^{-1})	UV/vis (nm)	color
8a	2076	370[a]	orange	1976	484, 531[a]	red
8b	2068	320[a]	green	no clear bands		green
8c	2064	352[a]	orange	1984	484, 532[a]	red
8d	2063	386,[a] 489	orange	1984	499, 525,[a] 544	red
8e	2059	387	orange	1961	500, 590[a]	violet
9a	2075	362	orange	1977	522, 544	red
9b	2065	330	green	no clear bands		green
9c	2063	368	orange	1969	510, 545	red
9d	2061	394,500	orange	1968	510, 545	red
9e	2061	399	orange	1963	500, 545	purple
3a	2035	388	orange	1934	474, 538, 770	red
3c	2030	401	orange	1934	475, 540, 774	red

[a] UV absorbances compared with theoretical λ_{max} values.

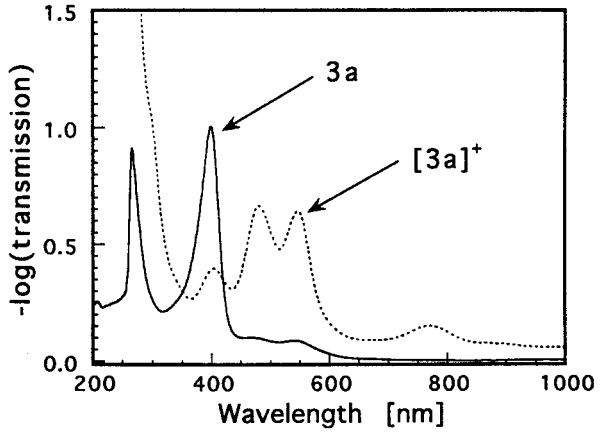

Figure 4. UV/vis spectra of **3a** and [**3a**]$^+$ in CH_2Cl_2.

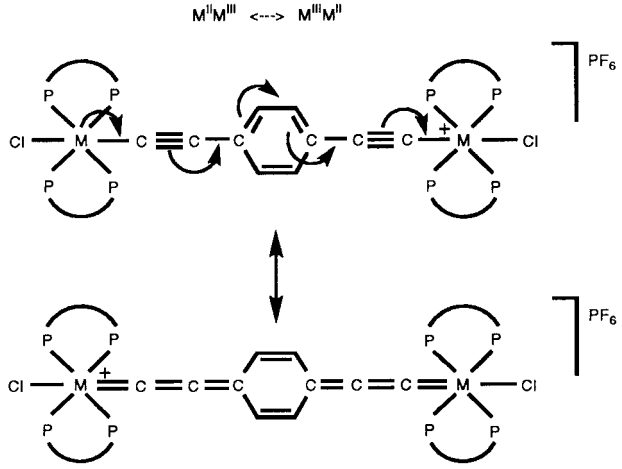

Figure 5. Limiting structures of the mixed-valence dinuclear species.

The intense IR stretching frequencies (1934−1984 cm^{-1}) and the colors of the mixed-valence species are associated with a delocalized limiting structure, which lies between that of an acetylide (2030−2076 cm^{-1}) and an allenylidene (1900−1940 cm^{-1}) form of the complexes (Figure 5). This proposal is supported by studies carried out on a ($Ru^{II}Fe^{III}$) mixed-valence system by Sato *et al.*[17] and by our investigations of some analogous ferrocenyl−ruthenium complexes.[22]

The synthesis of complexes [Cl(dppm)$_2$M(=C=C=CHPh)][PF_6] (**10**, M = Ru; **11**, M = Os) indicates that the ruthenium and osmium centers of the dinuclear complexes can form an allenylidene system. The color (red) and IR stretching frequency (1940 cm^{-1}) of **10** and **11** are similar to those of the mixed-valence species, implying that the latter exist in a delocalized allenylidene form. The existence of this allenylidene mixed-valence form suggests that upon oxidation of the dinuclear system, quinoid formation in the bridging ligand occurs; this could help to explain why the thiophene-containing complexes **8e** and **9e** give the largest K_{com} value and why those of complexes **8b** and **9b** are so low compared with the values for **8a** and **9a**.

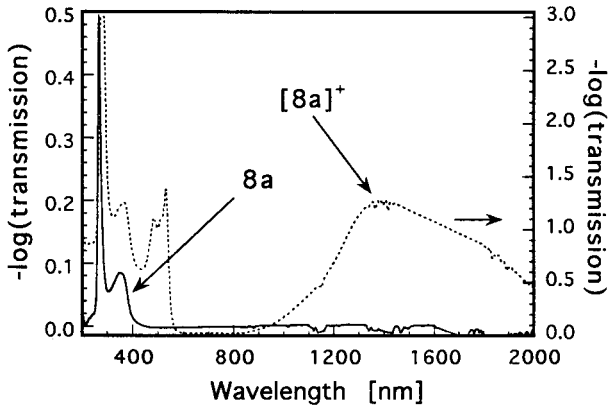

Figure 6. Electronic spectra of **8a** (*x* axis, absorbance (0.0−0.5); *y* axis, wavelength (250−2000 nm)) and [**8a**]$^+$ (*x* axis, absorbance (0.0−3.0); *y* axis, wavelength (250−2000 nm)).

Optical Absorbance Spectra of Dinuclear Metal Acetylides. The mixed-valence analogues of complexes **3a**, **8a**−**e**, and **9a**−**c** were electrosynthesized by bulk electrolysis. Comparison of the electronic spectra of the mixed-valence species [**3a**]$^+$, [**8a**−**e**]$^+$, and [**9a**−**c**]$^+$ with those of the neutral complexes shows the existence of a very broad and weak intervalence charge-transfer band (IVCT) in the near-infrared (near-IR) region of the spectrum, as well as two metal−ligand charge-transfer bands below 860 nm (Figure 6). The optical absorbance energies and the calculated $\Delta\nu_{1/2}$ values are detailed in Table 4. It was noted that the IVCT bands for the mixed-valence species were only observed at solution concentrations of at least 1×10^{-3} M, as has been similarly observed for [(C_5Me_5)Fe(CO)$_2$C≡CC≡C−Fe(dppe)(C_5Me_5)]PF_6.[21]

Treatment of the data in Table 4 by Hush theory relates the observed $\Delta\nu_{1/2}$ to the energy of the IVCT

(22) Colbert, M. C. B.; Lewis, J.; Long, N. J.; Raithby, P. R.; White, A. J. P.; Williams, D. J. *J. Chem. Soc., Dalton Trans.* **1997**, 99.

Table 4. Intervalence Charge Transfer (IVCT) Band Energies and Related Data

complex	ν_{max}[a] (cm^{-1})	$\Delta\nu_{1/2}$ (cm^{-1})	$\Delta E_{1/2}$ (V)	ν_o^{calc} (cm^{-1})	$\Delta\nu_{1/2}^{calc}$ (cm^{-1})	$10^3\alpha^2$
[**3a**]$^+$	6975	2000	0.16	1280	3630	2.0
[**8a**]$^+$	7334	2961	0.30	2400	3376	4.4
[**8b**]$^+$	none		0.19			
[**8c**]$^+$	7388	3167	0.33	2640	3312	6.5
[**8d**]$^+$	6655	2897	0.32	2560	3075	4.9
[**8e**]$^+$	8738	3460	0.36	2880	3679	8.9
[**9a**]$^+$	7850	2880	0.30	2400	3548	4.2
[**9b**]$^+$	none		0.17			
[**9c**]$^+$	8038	3064	0.30	2400	3608	4.6

[a] Samples run as CH_2Cl_2 solutions with a base line transmission of 0.06. Conditions and definitions: concentration 1×10^{-3} M, path length 2 mm; r = distance between metals, 12.2 Å for Ru and Os complexes, 12.0 Å for Fe species; $\Delta E_{1/2} = 0.1$ V, $\nu_o = 800$ cm^{-1}.

transition ν_{max} by eq 2, where ν_o is the internal energy difference between the two oxidation-state isomers (Mn^{I}-Fe^{II} and $Mn^{I}Fe^{III}$).[11] If one neglects ΔS (the entropy

$$\nu_{max} - \nu_o = (\Delta\nu_{1/2})^2/2310\ cm^{-1} \qquad (2)$$

change), then $\nu_o = \Delta G$ (free energy change). According to Taube's treatment of oxidized $[FcCNRu(NH_3)_5]$,[23] an upper limit to the value of ν_o (ΔG) can be estimated from the difference in the redox potentials ($\Delta E_{1/2}$) of the two metal centers ($\Delta E_{1/2}$ of 0.1 V corresponds to a ν_o value of *ca.* 8×10^2 cm^{-1}).

Taking $\Delta E_{1/2}$ from Table 1, we calculated the ν_o value for the complexes in Table 4. The ratio between the observed and calculated $\Delta\nu_{1/2}$ values is approximately 0.9 for the ruthenium and osmium analogues, this value being similar to that reported for class II mixed-valence species.[24] The delocalization parameter α^2 can be measured using eq 3, where r (Å) is the distance between the metals and ϵ_{max} is the molar absorptivity (M^{-1} cm^{-1}).

$$\alpha^2 = [(4.2 \times 10^{-4})\epsilon_{max}\Delta\nu_{1/2}]/\nu_{max}r^2 \qquad (3)$$

The value $r = 12.2$ Å is assumed to be the same for the ruthenium and osmium complexes examined here. It is taken as twice the distance from the ruthenium metal to the center of the phenyl ring in the previously reported complex $[Ru(dppm)_2(C{\equiv}CPh)_2]$.[25] The r value for the iron system is taken as being 12.0 Å, which is the equivalent measurement in the complex $[FeCl(dmpe)_2(C{\equiv}CPh)]$.[26] The resulting α^2 values calculated for the mixed-valence complexes are shown in Table 4. The range of these values indicates that the extent of electron delocalization in complexes [**3a**]$^+$, [**8a**−**e**]$^+$, and [**9a**−**c**]$^+$ depends greatly on the extent of metal−ligand interaction. Classification shows that all species belong to the Robin−Day "class II" mixed-valence systems.[19]

In conclusion, the α^2 values show the same trend as the electrochemically derived K_{com} values. The ruthenium complexes have slightly larger α^2 values than their osmium counterparts, suggesting that the metal−ligand interaction is greatest in the ruthenium species. This indicates that the bridging acetylide ligand must be acting as a donor ligand in accordance with studies by Kaim *et al.*,[27] which indicate that donor bridging ligands interact more favorably with π-accepting metal centers (*i.e.* Ru^{III} is a better π-acceptor than Os^{III}).

Within the ruthenium system, α^2 increases as follows with respect to the bridging ligand: **e** > **c** > **d** > **a**. This suggests that the thiophene bridging ligand interacts most favorably with the Ru^{III} center, thus allowing the greatest degree of metal−metal interaction and formation of its mixed-valence quinoid form.

The most important observation in these experiments, however, is the fact that complexes [**8b**]$^+$ and [**9b**]$^+$ do not exhibit IVCT bands in the near-IR region of the optical absorption spectra, despite having multiwave cyclic voltammograms (CV) (which suggests a degree of metal−metal interaction). This is explained by the fact that the 1,3-benzenediyl bridging ligand cannot form the quinoid mixed-valence structure.

Theoretical Calculations on Dinuclear Metal Acetylides. To understand the electrochemical behavior and the values of the comproportionation constants measured for the dinuclear ruthenium-bridged acetylides (**8a**,**b**,**d**,**e**) described in Table 2, as well as the spectrochemical properties of the neutral and charged complexes presented in Tables 3 and 4, it was necessary to examine the theoretical energies of the systems. The methods of calculation used for this purpose were (1) the combined Hartree−Fock semiempirical INDO (intermediate neglect of differential overlap)[28] method with an SCI (single configuration interaction) approach, for the electronic structure, and (2) combined Hartree−Fock semiempirical MNDO (modified neglect of differential overlap),[29] for the geometric structure calculations.

The first step in the calculations was to optimize the geometric structure of the bridging acetylide ligands in the neutral (L) and charged forms (L^+). The results of this optimization are shown in Figure 7; these indicate that the conjugated bridging system undergoes a structural change when an electron is removed. This change seems to indicate a loss of aromaticity of the central ring and the formation of a more quinoid-like geometry.

The theoretical electronic structure was then calculated for the neutral and charged ligand systems and for the charged dinuclear system. The relative ease of oxidation of each dinuclear system was related to the calculated ionization potential (IP_{calc}), which was predicted from the electronic structure using Koopman's theorem (the energy of the HOMO is directly related to the IP of a species). The stability of each system with respect to each other was related to the relative λ_{max} values (λ_{max} is the energy transition from the singlet ground-state HOMO to the singlet excited LUMO, $S_o \rightarrow S_1$; Figure 8). The most relevant results from the electronic spectra are described in Table 5.

The trend in IP_{calc} values clearly agrees with the first electrode potential ($E_{1/2}^{I}$) measured for each sample, in that the order of ease of oxidation is 2,5-thiophenediyl (**e**) < 1,4-benzenediyl (**a**) < 2,5-pyridinediyl (**d**) < 1,3-

(23) Dowling, N.; Henrey, P. N.; Lewis, N. A.; Taube, H. *Inorg. Chem.* **1981**, *20*, 2345.
(24) Colbran, S.; Robinson, B. H.; Simpson, J. *Organometallics* **1983**, *2*, 943.
(25) Hodge, A. J.; Lewis, J.; Long, N. J.; Page, N. A.; Parker, D. G.; Raithby, P. R.; White, A. J. P.; Williams, D. J. *J. Organomet. Chem.*, in press.
(26) Field, L. D.; George, A. V.; Hambley, T. W. *Inorg. Chem.* **1990**, *29*, 4565.
(27) Kaim, W.; Kasack, V. *Inorg. Chem.* **1990**, *29*, 4696.
(28) Ridley, J.; Zerner, M. *Theor. Chim. Acta* **1974**, *33*, 35.
(29) Dewer, M. J. S.; Thiel, W. *J. Am. Chem. Soc.* **1977**, *99*, 1499.

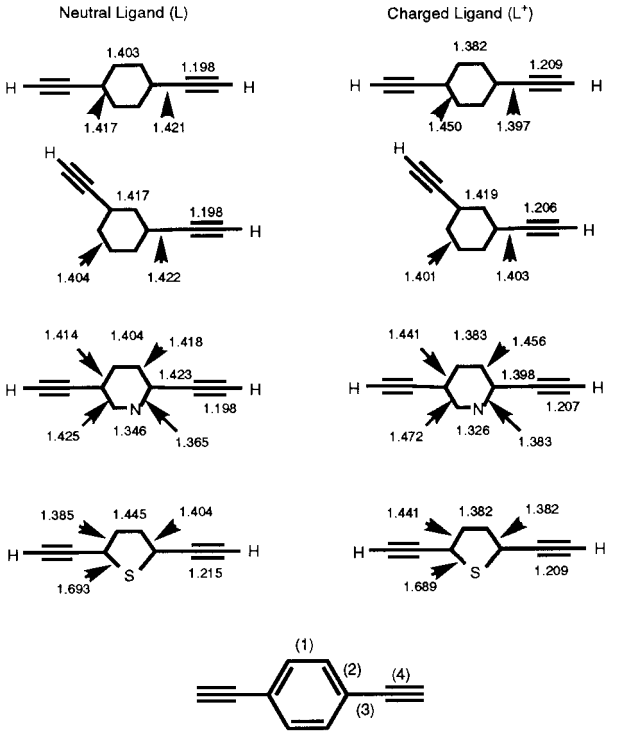

Comparison of the geometry of the neutral ligand (L) and the charged ligand (L^+) shows shortening of bonds (1) and (3) and lengthening of (2) and (4). This suggests that the charged ligands are more quinoid than aromatic in structure.

Figure 7. Geometric optimization of neutral and charged acetylide ligands.

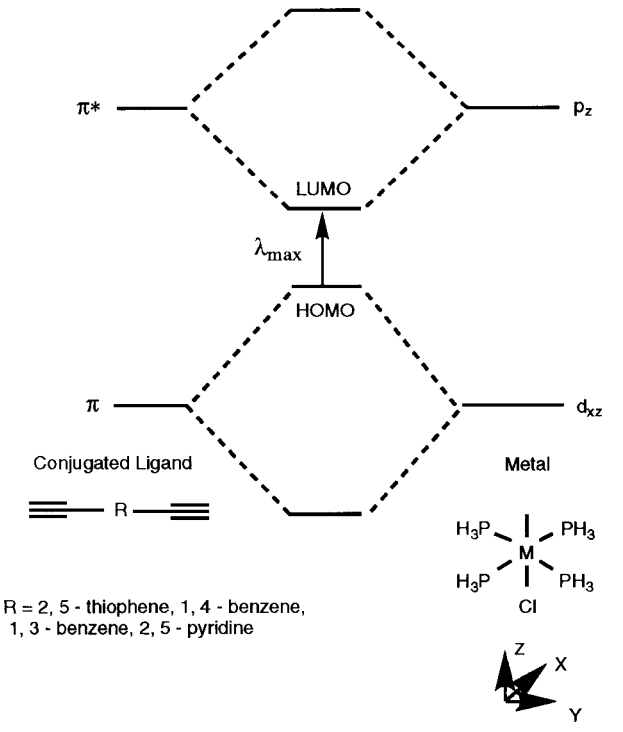

Figure 8. MO diagram for the interaction of the $M(PH_3)_4Cl$ fragment and the bridging acetylide ligand. The acetylide ligand approaches along the *z* axis; phosphines approach along the *xy* axis.

benzenediyl (**b**). The optical absorption energies (eV) from the UV spectra of the $M^{II}M^{II}$ and $M^{II}M^{III}$ complexes are also in good agreement with the theoretical λ_{max} values (eV). The differences between the theoretical λ_{max}^{calc} and the measured UV absorbance energies could be attributed to the fact that the model system is set up with the metal coordinated to four identical monodentate phosphines (PH_3) and not two dppm ligands as in the experimentally investigated systems.

Both these correlations suggest that the model for the system is essentially correct. The prediction of a quinoid-type interaction in the mixed-valence system is supported by the results in that (i) the thiophene bridging ligand complex has the lowest $E_{1/2}^{I}$ and λ_{max} values, as it forms the quinoid geometry more easily than the other bridging ligands in stabilizing the $M^{II}M^{III}$ species, and (ii) complex **8b** has a very high $E_{1/2}^{I}$ value with respect to that of **8a** and does not show a significant UV (color) change when it is oxidized from $M^{II}M^{II}$ to $M^{II}M^{III}$.

This latter observation is probably because the 1,3-benzenediyl spacer cannot form a quinoid geometry to stabilize the mixed-valence complex. The redox chemistry and UV data of the osmium analogues of the ruthenium $M^{II}M^{II}$ and $M^{II}M^{III}$ systems obey the same trends and are thus further support for the presented theoretical model.

Experimental Section

General Comments. All preparations were carried out using standard Schlenk techniques.[30] All solvents were distilled over standard drying agents under nitrogen directly before use, and all reactions were carried out under an atmosphere of nitrogen. Alumina gel (type UG-1) and silica gel (230−400 mesh) were used for chromatographic separations.

All NMR spectra were recorded on Bruker instruments, operating at either 250.1 or 400.1 MHz (^1H), 62.9 MHz ($^{13}C\{^1H\}$), and 101.3 MHz ($^{31}P\{^1H\}$). Chemical shifts are reported in δ using $CDCl_3$ (^1H, δ 7.25 ppm; ^{13}C, δ 77.0 ppm) as the reference for ^1H and $^{13}C\{^1H\}$ spectra, while the $^{31}P\{^1H\}$ spectra were referenced to trimethyl phosphite. Infrared spectra were recorded in NaCl solution cells (CH_2Cl_2) using a Perkin-Elmer 1710 Fourier transform IR spectrometer. UV/vis spectra were recorded on a Perkin-Elmer Lambda 9 spectrometer using CH_2Cl_2 solutions. Mass spectra were recorded using positive FAB methods, on a Kratos MS60 spectrometer. Microanalyses were carried out at the Department of Chemistry, University of Cambridge. The electrochemical responses were recorded using an Autolab PGSTAT 20 potentiostat with a standard three-electrode system (platinum working and auxiliary electrodes and Ag/AgCl or calomel reference electrodes). The electrochemical experiments were measured at 298 K using a 0.1 M $[NBu_4][BF_4]/CH_2Cl_2$ (solvent dried over CaH_2) solution as supporting electrolyte, and all solutions were N_2-purged. All electrochemical measurements were referenced against the ferrocene/ferrocenium redox couple ($E_{1/2} = 0.50$ V vs Ag at 298 K in 0.1 M $[NBu_4][BF_4]/CH_2Cl_2$).

Starting Materials. The metal halides *trans*-$[Fe(depe)_2Cl_2]$,[26] *trans*-$[Fe(dmpe)_2Cl_2]$,[31] *cis*-$[Ru(dppm)_2Cl_2]$,[32,33] and *cis*-$[Os(dppm)_2Cl_2]$[31] were synthesized using published procedures. The diacetylide ligands 1,4-diethynylbenzene (**2a**), 1,3-diethynylbenzene (**2b**), 2,5-diethynyl-*p*-xylene (**2c**), 2,5-diethynylpy-

(30) Shriver, D. F. In *Manipulation of Air-Sensitive Compounds*; McGraw-Hill: New York, 1969.
(31) Kovacia, P.; O'Brace, N. *Inorg. Synth.* **1960**, *4*, 172.
(32) Chatt, J.; Hayter, R. G. *J. Chem. Soc., Dalton Trans.* **1961**, 896.
(33) (a) Chaudret, B.; Commenges, G.; Poiblanc, R. *J. Chem. Soc., Dalton Trans.* **1984**, 1635. (b) Evans, I. P.; Spencer, A.; Wilkinson, G. *J. Chem. Soc., Dalton Trans.* **1973**, 204.

Table 5. Experimental and Theoretical Comparison of Electrochemical and Spectroscopic Data

complex	$IP_{calc}(M^{II}M^{II})$ (eV)	$E_{1/2}{}^{I}(M^{II}M^{II})$ (V)	$\lambda_{max}{}^{calc}(M^{II}M^{II})$ (eV)	$UV(M^{II}M^{III})$ (eV)	$\lambda_{max}{}^{calc}(M^{II}M^{III})$ (eV)	$UV(M^{II}M^{III})$ (eV)
8a	4.67	0.27	3.51	3.35	2.41	2.34
8b	5.17	0.46	3.93	3.88	3.91	none
8d	4.73	0.36	3.24	3.21	2.49	2.28
8e	4.43	0.10	3.12	3.20	2.13	2.10

Table 6. Analytical Data for Dinuclear Metal Acetylides

complex	IR (cm^{-1})	^{31}P NMR (ppm)	M^+ calc (amu)	M^+ found (amu)	anal. calcd (%)[a]	anal. found (%)
8a	2076	−147.5	1933	1935	C, 67.73; H, 4.68	C, 67.64; H, 4.66
8b	2068	−147.3	1933	1935	C, 67.73; H, 4.68	C, 67.34; H, 4.58
8c	2064	−147.3	1961	1963	C, 67.38; H, 4.84	C, 66.97; H, 4.79
8d	2063	−147.5	1934	1937	C, 66.48; H, 4.66	C, 66.41; H, 4.70
8e	2059	−147.9	1940	1942	C, 61.23;[b] H, 4.28[b]	C, 61.52; H, 4.33
9a	2075	−190.2, −193.3	2113	2113	C, 61.57; H, 4.32	C, 61.43; H, 4.28
9b	2065	−189.7, −193.4	2113	2113	C, 61.57; H, 4.32	C, 61.33; H, 4.37
9c	2063	−189.7, −193.2	2141	2142	C, 61.88; H, 4.45	C, 61.66; H, 4.38
9d	2061	−189.1, −193.4	2114	2114	C, 60.99; H, 4.27	C, 60.84; H, 4.39
9e	2061	−190.1, −193.2	2119	2120	C, 56.50;[b] H, 3.95[b]	C, 56.31; H, 3.98

[a] The analyses were calculated with the inclusion of 0.5 mol of CH_2Cl_2 in each complex. [b] The figures were calculated and measured for the blue mixed-valence $[M^{II}M^{III}][PF_6]$ species.

ridine (**2d**), and 2,5-diethynylthiophene (**2e**) were synthesized by modified literature procedures[34,35] and were characterized by ^1H and $^{13}C\{^1H\}$ NMR and infrared spectroscopy. [(Ph)(OH)(H)C−C≡CH] was purchased from Aldrich Chemical Co.

Synthesis of Dinuclear Metal Acetylides. The dinuclear metal acetylides were synthesized using modifications of literature procedures for analogous iron,[12] ruthenium,[36] and osmium[36] species, and the complexes were characterized by microanalysis and infrared, mass, and NMR spectroscopy.

(i) *trans*-[Cl(depe)$_2$Fe−C≡CC$_6$H$_4$C≡C−Fe(depe)$_2$Cl] (3a). Freshly sublimed **2a** (0.025 g, 0.20 mmol) was added to a solution of freshly cut sodium (0.005 g, 0.22 mmol) in methanol (2 mL). This mixture was then added dropwise to [Fe(depe)$_2$Cl$_2$] (0.15 g, 0.40 mmol) in methanol (10 mL). After 1 min, a brown precipitate appeared and the mixture was stirred for another 30 min. **3a** was filtered off as a brown solid and washed with cold methanol (2 × 5 mL); it required no further purification (0.07 g, 32%). Anal. Calcd for $[C_{50}H_{100}P_8Cl_2Fe_2]$: C, 53.1; H, 8.8. Found: C, 52.8; H, 8.6. IR (ν (cm^{-1}), C≡C): 2030. ^1H NMR (400 MHz, C_6H_6): δ 1.79 (s br, 16H, CH_2), 2.27 (s br, 48H, CH_3), 2.45 (m, 32H, CH_2), 7.34 (m, 4H, CH). $^{31}P\{^1H\}$ NMR (CD_2Cl_2, 101.3 MHz): δ −100 (s br, $P(C_2H_5)_2$). MS (FAB + ve): *m*/*z* 1130.3 (M^+, 31) calcd M^+ 1130.0.

(ii) *trans*-[Cl(dmpe)$_2$Fe−C≡CC$_6$H$_2$(CH$_3$)$_2$C≡C−Fe(dmpe)$_2$Cl] (3c). [Fe(dmpe)$_2$Cl$_2$] (0.15 g, 0.35 mmol) was reacted with **2c** (0.027 g, 0.17 mmol) using a procedure analogous to that above, to yield a light brown solid (**3c**; 0.17 g, 53%). Anal. Calcd for $[C_{36}H_{72}P_8Cl_2Fe_2]$: C, 46.2; H, 7.7. Found: C, 45.9; H, 7.6. IR (ν (cm^{-1}), C≡C): 2035. ^1H NMR (400 MHz, C_6H_6): δ 1.13 (s, 6H, CH_3), 1.54 (s br, 48H, CH_3), 1.72 (s br, 16H, CH_2), 7.41 (m, 2H, CH). $^{31}P\{^1H\}$ NMR (CD_2Cl_2, 101.3 MHz): δ −104 (s br, $P(C_2H_5)_2$). MS (FAB + ve): *m*/*z* 935.5 (M^+, 38), calcd M^+ 935.2.

(iii) *trans*-[Cl(dppm)$_2$M(C≡CRC≡C)M(dppm)$_2$Cl] (8a−d, 9a−d). The following procedure was used to synthesize complexes **8a**−**d** and **9a**−**d**. In each case, 2 equiv of *cis*-[M(dppm)$_2$Cl$_2$] (**4**, M = Ru; **5**, M = Os) was treated with 1 equiv of the diacetylene **2a**−**d**. The intermediate vinylidenes were not characterized but were reacted *in situ* to yield the dinuclear metal acetylides in yields of *ca.* 50%. The physical data for each complex are presented in Table 6.

cis-[M(dppm)$_2$Cl$_2$] (0.3 mmol) was added to HC≡CRC≡CH (0.15 mmol) and $NaPF_6$ (0.6 mmol) in CH_2Cl_2 (25 mL) and stirred for 8 h (24 h for the osmium complexes **9a**−**d**). The dark orange solution was filtered to remove any excess $NaPF_6$ and NaCl byproduct, and DBU (0.3 mmol) was added to the vinylidene solution and the stirring continued for a further 2 h. The resulting yellow solution was filtered and the solvent removed *in vacuo*. The solid residue was washed with acetone (2 × 10 mL) and then redissolved in a CH_2Cl_2/hexane two-layer system, and slow recrystallization allowed isolation of the product as a fine yellow powder. Further purification was accomplished by washing this solid with acetone (1 × 10 mL), and each complex was formed in *ca.* 50% yield.

(iv) *trans*-[Cl(dppm)$_2$M(C≡CC$_4$H$_2$SC≡C)M(dppm)$_2$Cl] (8e, 9e). *cis*-[M(dppm)$_2$Cl$_2$] (0.3 mmol) was added to freshly prepared **2e** (0.15 mmol) and $NaPF_6$ (0.6 mmol) in CH_2Cl_2 (25 mL), and the mixture was stirred for 24 h. The resultant dark blue-black vinylidene solution was filtered, and DBU (0.3 mmol) was added. After it was stirred for a further 2 h, the solution was filtered and the solvent removed *in vacuo*. The crude solid was washed with acetone (2 × 10 mL), and recrystallization from a CH_2Cl_2/hexane two-layer system afforded a microcrystalline yellow powder in *ca.* 25% yield.

Synthesis of Allenylidene Complexes. (i) [(dppm)$_2$ClRu=C=C=CHPh][PF$_6$] (10). *cis*-[M(dppm)$_2$Cl$_2$] (0.40 g, 0.43 mmol) was added to [(Ph)(OH)(H)CC≡CH] (0.06 g, 0.46 mmol) and $NaPF_6$ (0.15 g, 0.89 mmol) in CH_2Cl_2 (25 mL) and stirred for 20 h at room temperature. The deep red solution was filtered to remove any excess $NaPF_6$ and NaCl byproduct, and the solvent was removed *in vacuo* to yield a fine red solid (**10**; 0.47 g, 93%). The solid was washed with cold benzene (2 × 10 mL) and then recrystallized from a CH_2Cl_2/hexane two-layered system. Anal. Calcd for $[C_{59}H_{50}P_4ClRu][PF_6]$: C, 60.14; H, 4.30. Found: C, 60.31; H, 4.27. IR (ν (cm^{-1}), C≡C): 1943. ^1H NMR (250.1 MHz, $CDCl_3$): δ 5.28 (m, 4H, PCH_2P), 6.68−7.55 (m, 45H, PC_6H_5), 8.55 (t, 1H, C=CH). $^{13}C\{^1H\}$ NMR (62.9 MHz, $CDCl_3$): δ 45.9 (PCH_2P), 128−133 (PC_6H_5), 142.2 (*C*=C), 151.0 (C=*C*), 216.0 (Ru=*C*). $^{31}P\{1H\}$ NMR (CD_2Cl_2, 101.3 MHz): δ −155.6 (s, $CH_2PC_6H_5$). MS (FAB + ve): *m*/*z* 1020 (M^+, 47), calcd M^+ 1018.6.

(ii) [(dppm)$_2$ClOs=C=C=CHPh][PF$_6$] (11). The synthetic procedure for **10** was followed and afforded a dark red solid (**11**; 0.48 g, 88%). Anal. Calcd for $[C_{59}H_{50}P_4ClOs][PF_6]$: C, 55.52; H, 3.99. Found: C, 55.78; H, 3.92. IR (ν (cm^{-1}), C≡C): 1940. ^1H NMR (250.1 MHz, $CDCl_3$): δ 5.70 (m, 2H, PCH_2P), 6.12 (m, 2H, PCH_2P), 6.86−7.38 (m, 45H, PC_6H_5), 11.7 (t, 1H, C=CH). $^{13}C\{^1H\}$ NMR (62.9 MHz, $CDCl_3$): δ 45.9

(34) Takahashi, S.; Kuroyama, Y.; Sonogashira, K.; Hagihara, N. *Synth. Commun.* **1980**, 627.
(35) Austin, W. B.; Bilow, N.; Kelleghan, W. J.; Law, K. S. Y. *J. Org. Chem.* **1981**, *46*, 2280.
(36) Haquette, P.; Pirio, N.; Touchard, D.; Toupet, L.; Dixneuf, P. H. *J. Chem. Soc., Chem. Commun.* **1993**, 163.

(PCH_2P), 128−133 (PC_6H_5), 144.4 (*C*═C), 147.9 (C═*C*), 230.0 (Ru═*C*). $^{31}P\{^1H\}$ NMR (CD_2Cl_2, 101.3 MHz): δ −199.1 (s, $CH_2PC_6H_5$). MS (FAB + ve): *m*/*z* 1109.4 (M^+, 38), calcd M^+ 1107.6.

X-ray Crystallography. Crystal Structure Determination. Crystal data for **10**: $[C_{59}H_{50}P_4ClRu][PF_6]$, M_r = 1164.4, tetragonal, space group *I*4/*m*, $a = b = 34.579(3)$ Å, $c = 18.437(3)$ Å, $V = 22045(4)$ Å^3, $Z = 16$ (there are two crystallographically independent C_s-symmetric molecules in the asymmetric unit), $D_c = 1.40$ g cm^{-3}, μ(Mo Kα) = 5.36 cm^{-1}, $F(000) = 9504$. A deep red octagonal prism of dimensions 0.33 × 0.28 × 0.27 mm was used.

Data Collection and Processing. Data were measured on a Siemens P4/PC diffractometer with Mo Kα radiation (graphite monochromator) using ω scans. A total of 10 470 independent reflections were measured ($2\theta \leq 50°$), of which 6444 had $|F_o| > 4\sigma(|F_o|)$ and were considered to be observed. The data were corrected for Lorentz and polarization factors, but not for absorption.

Structure Analysis and Refinement. The structure was solved by direct methods. A ΔF map revealed rotational disorder (55:45) in one of the phenyl rings of one of the independent molecules. All the major occupancy non-hydrogen atoms of the two independent C_s-symmetric molecules were refined anisotropically, the phenyl rings being treated as optimized rigid bodies. The PF_6 anions are distributed over four partial-occupancy sites within the asymmetric unit, and of these, two are disordered. The nondisordered atoms of the PF_6 anions were refined anisotropically. The minor occupancy atoms of the disordered phenyl ring and the disordered PF_6 atoms were refined isotropically. The positions of the hydrogen atoms were idealized, assigned isotropic thermal parameters ($U(H) = 1.2U_{eq}(C)$), and allowed to ride on their parent carbon atoms. Refinement was by full-matrix least squares based on F^2 to give $R_1 = 0.076$ and w$R_2 = 0.184$ for the observed data and 562 parameters. The maximum and minimum residual electron densities in the final ΔF map were 1.61 and −1.69 e Å^{-3}, respectively, in the region of the disordered PF_6 anions. The mean and maximum shift/error ratios in the final refinement cycle were 0.001 and 0.021, respectively.

Computations were carried out on a 50 MHz 486 PC computer using the SHELXTL PC program system.[37] Additional material available from the Cambridge Crystallographic Data Centre comprises fractional atomic coordinates, H-atom coordinates, thermal parameters, and complete bond lengths and angles.

Acknowledgment. We thank the EPSRC, the British Council, and the Leverhulme Trust (N.J.L., M.Y.) for financial support and Anna Köhler for helpful discussions.

Supporting Information Available: A figure giving another view of **10** and tables and text giving details of the X-ray structure determination of **10** (12 pages). Ordering information is given on any masthead page.

OM970130P

(37) SHELXTL PC version 5.03; Siemens Analytical X-ray Instruments, Inc., Madison, WI, 1994.